Journal of Physics: Conference Series **78** (2007) 012019 doi:10.1088/1742-6596/78/1/012019

Ab initio Hadron Structure from Lattice QCD

LHP Collaboration: J. D. Bratt[1], R. G. Edwards[2], M. Engelhardt[3], G. T. Fleming (presenter)[4,†], Ph. Hägler[5], B. Musch[5], J. W. Negele[1], K. Orginos[2,6], A. V. Pochinsky[1], D. B. Renner[7], D. G. Richards[2], W. Schroers[8]

[1] Center for Theoretical Physics, Massachusetts Institute of Technology, Cambridge, MA 02139, USA
[2] Jefferson Laboratory MS 12H2, 12000 Jefferson Avenue, Newport News, VA 23606, USA
[3] Department of Physics, New Mexico State University, Las Cruces, NM 88003, USA
[4] Sloane Physics Laboratory, Yale University, New Haven, CT 06520, USA
[5] Institut für Theoretische Physik T39, Physik-Department der TU München, James-Franck-Straße, D-85747 Garching, Germany
[6] Department of Physics, College of William and Mary, Williamsburg, VA 23187, USA
[7] Department of Physics, University of Arizona, Tucson, AZ 85721, USA
[8] John von Neumann-Institut für Computing NIC/DESY, D-15738 Zeuthen, Germany

E-mail: [†]George.Fleming@Yale.edu

Abstract. Early scattering experiments revealed that the proton was not a point particle but a bound state of many quarks and gluons. Deep inelastic scattering (DIS) experiments have accurately determined the probability of struck quarks carrying a fraction of the proton's momentum. The current generation of experiments and Lattice QCD calculations will provide detailed multi-dimensional pictures of the distributions of quarks and gluons inside the proton.

1. A Brief History of Hadron Structure

In 1904, J. J. Thomson proposed the *plum pudding model* [1] of atomic structure where electron "plums" were surrounded by a diffuse positively charged "pudding". In 1909, Geiger and Marsden [2], working under E. Rutherford, observed hard scattering of α particles on very thin gold films. In 1911, Rutherford's analysis [3] of the *Geiger-Marsden experiment* showed the hadronic nucleus was orders of magnitude smaller than the atom, possibly even point-like.

In 1931, Stern and collaborators measured the anomalous magnetic moment of the proton [4, 5], providing the first evidence that nucleons were more than mere point-like Dirac particles. In 1950, Rosenbluth proposed a formalism [6] for extracting the spatial distributions (called *form factors*) of the proton's charge and the magnetic moment in proton-electron elastic scattering experiments. In 1955, Hofstadter and McAllister made the first measurements of the rms radius for the charge and magnetic moment of the proton and neutron [7, 8, 9, 10]

In 1967, a *deep inelastic scattering* (DIS) experiment led by Friedman, Kendall and Taylor [11] revealed point-like constituents (called "partons") inside. The effect was analogous to the Geiger-Marsden experiment but at much higher energies. Bjorken soon realized that the probability of finding a parton depended primarily on the fraction of the proton's momentum carried by the struck parton, x. These 1-D functions are called *parton distribution functions* (PDF's). By

1974, it was widely understood that the quarks and gluons of quantum chromodynamics (QCD) were the DIS partons.

In the mid-1990's, PDF's were generalized [12, 13, 14, 15] for processes where a removed parton with initial momentum fraction x_i is reinserted into the hadron with final momentum fraction x_f after receiving a momentum kick $\xi = x_f - x_i$. Generalized PDF's (GPD's) unify and extend the previously successful concepts of inelastic PDF's and elastic form factors and reveal a new dimension (2-D) to hadron structure. GPD's can be parameterized by their Mellin moments, called generalized form factors (GFF's). GPD's measured in different physical processes give distinct 2-D slices of the hadron. These include changing the initial spin of the target hadron or probe or measuring the spins of the struck parton, final state hadron or probe. By combining different 2-D slices, tomography can be used to produce a fully 3-D picture of hadron structure.

2. Momentum fraction

The $\mathcal{O}(p^2)$ covariant baryon chiral perturbation theory (CBChPT) result[16] for the isovector GFF $A_{20}^{u-d}(t)$ is

$$A_{20}^{u-d}(t,m_\pi) = A_{20}^{0,u-d}\left(f_A^{u-d}(m_\pi)+\frac{g_A^2}{192\pi^2 f_\pi^2}h_A(t,m_\pi)\right)+\widetilde{A}_{20}^{0,u-d}j_A^{u-d}(m_\pi)+A_{20}^{m_\pi,u-d}m_\pi^2+A_{20}^{t,u-d}t\,, \tag{1}$$

where $f_A^{u-d}(m_\pi)$, $h_A(t,m_\pi)$ and $j_A^{u-d}(m_\pi)$ contain the non-analytic dependence on the pion mass and momentum transfer squared and $A_{20}^{0,u-d} \equiv A_{20}^{u-d}(t=0,m_\pi=0)$. The lattice results are shown in Fig. 1 with additional curves that show the predicted pion mass dependence in the limit that the nucleon mass becomes very heavy.

The (total) isosinglet momentum fraction of quarks, $A_{20}^{u+d}(t=0) = \langle x\rangle_{u+d}$ is not only an important hadron structure observable on its own but is in addition an essential ingredient for the computation of the total angular momentum contribution of quarks to the nucleon spin, $J^{u+d} = 1/2(A_{20}^{u+d}(0) + B_{20}^{u+d}(0))$. The combined (t,m_π)-dependence in CBChPT is given by [16]:

$$\begin{aligned} &A_{20}^{u+d}(t,m_\pi) = \\ &\quad A_{20}^{0,u+d}\left(f_A^{u+d}(m_\pi)-\frac{g_A^2}{64\pi^2 f_\pi^2}h_A(t,m_\pi)\right)+A_{20}^{m_\pi,u+d}m_\pi^2+A_{20}^{t,u+d}t+\Delta A_{20}^{u+d}(t,m_\pi)+\mathcal{O}(p^3)\,, \end{aligned} \tag{2}$$

where $A_{20}^{0,u+d} \equiv A_{20}^{u+d}(t=0,m_\pi=0)$, and $f_A^{u+d}(m_\pi)$ and $h_A(t,m_\pi)$ contain the non-analytic dependence on the pion mass and momentum transfer squared. The lattice results are shown in Fig. 2 with additional curves that show the predicted pion mass dependence in the limit that the nucleon mass becomes very heavy.

3. Nucleon Isovector Ratio G_A/F_1

The axial charge of the nucleon can be measured quite accurately in neutron beta decay and can be accurately computed in Lattice QCD as well [17]. The elastic axial form factor is much more difficult to determine experimentally. In fact, the current empirical parameterization to which all experimental data is fitted

$$G_A(Q^2) = \frac{g_A}{\left(1+Q^2/M_A^2\right)^2} \tag{3}$$

is the same that was used by Hofstadter and McAllister [7, 8, 9, 10] to model electromagnetic elastic scattering in the 1950's. With more precise measurements in the 1960's and beyond of the electromagnetic form factors, more complicated empirical parameterizations are used to fit the

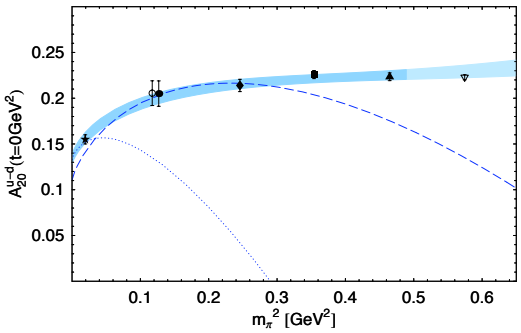

Figure 1. Lattice results for A_{20}^{u-d} at $t = 0$ GeV^2 versus m_π^2 together with a global chiral fit using Eq. (1), denoted by the error band and the phenomenological result from CTEQ6, indicated by the star. The heavy-baryon-limit of the CBChPT fit is shown by the dotted line.

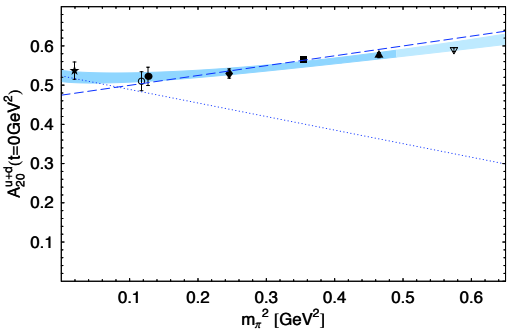

Figure 2. Lattice results for A_{20}^{u+d} at $t = 0$ GeV^2 versus m_π^2 together with the result of a global chiral fit using Eq. (2), denoted by the error band, and the phenomenological value from CTEQ6, denoted by a star. The heavy-baryon-limit of the CBChPT fit is shown by the dotted line.

available electromagnetic data [18, 19]. With the advent of current and next generation neutrino scattering experiments (MiniBooNE, K2K, NuMi, ...), the validity of dipole parameterization in Eq. (3) will finally be tested.

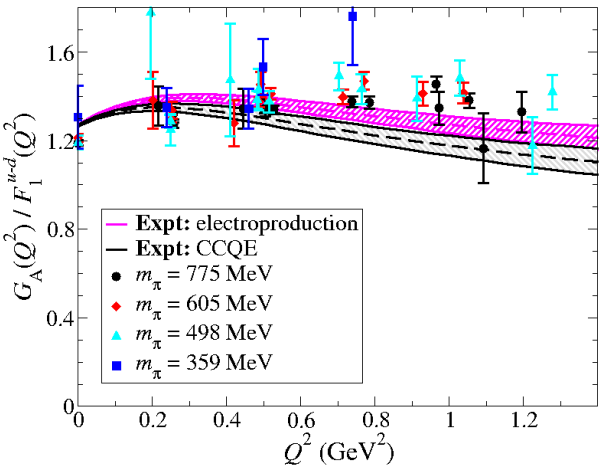

Figure 3. Ratio of the isovector part of the ratio of the nucleon axial form factor to the Dirac form factor for various pion masses in Lattice QCD. Experimental bands correspond to $M_A = 1.069(16)$ for electroproduction and $M_A = 1.026(21)$ for νCCQE [20]. The experimental Dirac form factor is derived from the empirical parameterization of J. J. Kelly [18].

In Fig. 3, Lattice QCD data is presented alongside bands representing the experimental situation last year. The lattice results favor higher values for the axial mass. A few weeks ago at the *Fifth International Workshop on Neutrino-Nucleus Interactions in the Few-GeV Region* [21], two experiments announced new measurements of the axial mass: MiniBooNE finds $M_A = 1.23 \pm 0.20$ [22] and K2K finds $M_A = 1.144 \pm 0.077\ ^{+0.078}_{-0.072}$ [23] with substantially more data that earlier experiments. Lattice QCD also favors this larger value for M_A.

4. Transverse quark distributions

As the momentum fraction increases, $x \to 1$, the average transverse position approaches the center of mass of the nucleon, $\langle b_\perp^2 \rangle^q \to 0$. GFF's are moments of the distribution of transverse quark positions.

$$A^q_{n0}(-\mathbf{\Delta}_\perp^2) = \int d^2b_\perp e^{i\mathbf{\Delta}_\perp \cdot \mathbf{b}_\perp} \int_{-1}^{1} x^{n-1} q(x, \mathbf{b}_\perp) \tag{4}$$

Moments of the rms transverse position are related to the slope of the GFF's

$$\left\langle b_\perp^2 \right\rangle^q_{(n)} = -4 \frac{A^{q\prime}_{n0}(0)}{A^q_{n0}(0)} \tag{5}$$

Higher moments A^q_{n0} are weighted towards $x \sim 1$. Fig. 4 shows the slope of A^q_{n0} decreases as n increases, confirming the current model picture of transverse quark distributions in Fig. 5.

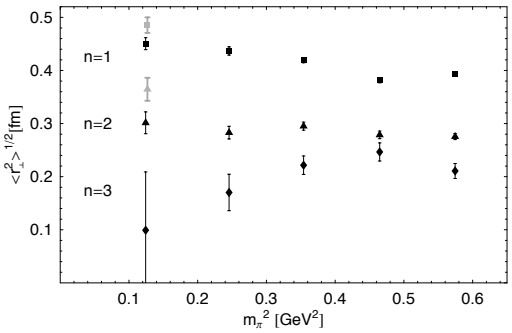

Figure 4. Two dimensional rms radii of the vector GFFs versus m_π^2 for the flavor combination $u - d$. The results for $m_\pi = 354$ MeV, $L^3 = 20^3$ are displayed in gray.

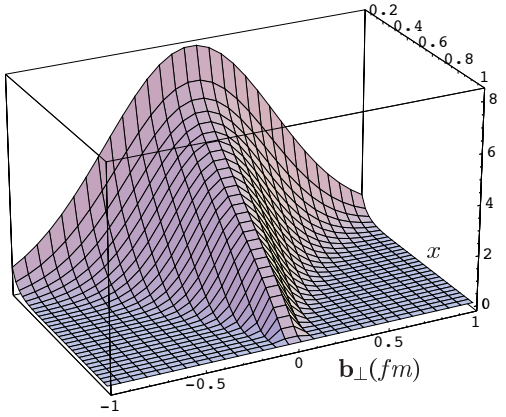

Figure 5. The model of M. Burkardt [24] for the distribution of transverse positions of quarks in the nucleon vs. their momentum fraction, $q(x, \mathbf{b}_\perp)$.

5. Quark contributions to nucleon spin

The Ji sum rule [25]

$$J^q = \frac{1}{2}\left(A^q_{20}(0) + B^q_{20}(0)\right), \qquad \frac{1}{2}\Delta\Sigma^q = \widetilde{A}^q_{10}(0), \qquad L^q = J^q - \frac{1}{2}\Delta\Sigma^q \tag{6}$$

allows for a gauge invariant decomposition of the quark angular momentum contributions to the nucleon spin. Fig 6 shows the combined intrinsic spin and orbital angular momentum contributions of the light up and down quarks. Taken together, the light quark orbital motion does not contribute to the spin of the nucleon.

Fig 7 shows separately the up and down quark contributions. The orbital angular momentum of up and down quarks, L^u and L_d, separately are relatively large but cancel in combination. Surprisingly, the orbital and spin contributions of the down quarks, L^d and $\frac{1}{2}\Delta\Sigma^d$ are consistent with equal magnitude and opposite sign. The physical origin of these surprising features is not well understood.

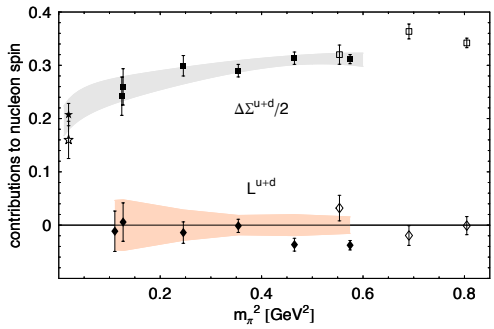

Figure 6. Total quark spin and orbital angular momentum contributions to the spin of the nucleon. The filled and open stars represent values given in HERMES 2007 [26] and 1999 [27] respectively and open symbols represent earlier LHPC/SESAM calculations. The error bands are explained in the text. Disconnected contributions are not included.

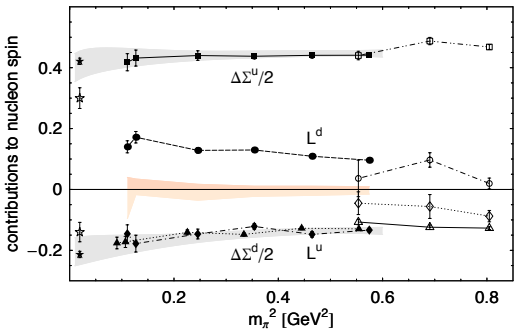

Figure 7. Quark spin and orbital angular momentum contributions to the spin of the nucleon for up and down quarks. The filled and open stars represent values given in HERMES 2007 [26] and 1999 [27] respectively and open symbols represent earlier LHPC/SESAM calculations. The error bands are explained in the text. Disconnected contributions are not included.

References

[1] Thomson J J 1904 *Phil. Mag.* **7** 237–265
[2] Geiger H and Marsden E 1909 *Proc. Roy. Soc. Lond. A Math. Phys. Eng. Sci.* **82** 495–500
[3] Rutherford E 1911 *Phil. Mag.* **21** 669–688
[4] Estermann I, Frisch R and Stern O 1932 *Z. Phys.* **73** 348–365
[5] Estermann I, Frisch R and Stern O 1933 *Nature* **132** 169
[6] Rosenbluth M N 1950 *Phys. Rev.* **79** 615–619
[7] Hofstadter R and McAllister R W 1955 *Phys. Rev.* **98** 217–218
[8] McAllister R W and Hofstadter R 1956 *Phys. Rev.* **102** 851–856
[9] Hofstadter R 1956 *Rev. Mod. Phys.* **28** 214–254
[10] Hofstadter R 1957 *Ann. Rev. Nucl. Part. Sci.* **7** 231–316
[11] Coward D H *et al.* 1968 *Phys. Rev. Lett.* **20** 292–295
[12] Müller D, Robaschik D, Geyer B, Dittes F M and Horejsi J 1994 *Fortschr. Phys.* **42** 101 (*Preprint* `hep-ph/9812448`)
[13] Ji X D 1997 *Phys. Rev.* **D55** 7114–7125 (*Preprint* `hep-ph/9609381`)
[14] Radyushkin A V 1997 *Phys. Rev.* **D56** 5524–5557 (*Preprint* `hep-ph/9704207`)
[15] Diehl M 2003 *Phys. Rept.* **388** 41–277 (*Preprint* `hep-ph/0307382`)
[16] Dorati M, Gail T A and Hemmert T R 2007 (*Preprint* `nucl-th/0703073`)
[17] Edwards R G *et al.* (LHPC) 2006 *Phys. Rev. Lett.* **96** 052001 (*Preprint* `hep-lat/0510062`)
[18] Kelly J J 2004 *Phys. Rev.* **C70** 068202
[19] Bradford R, Bodek A, Budd H and Arrington J 2006 *Nucl. Phys. Proc. Suppl.* **159** 127–132 (*Preprint* `hep-ex/0602017`)
[20] Bernard V, Elouadrhiri L and Meissner U G 2002 *J. Phys.* **G28** R1–R35 (*Preprint* `hep-ph/0107088`)
[21] Cavanna F and Morfin J 2007 Fifth international workshop on neutrino-nucleus interactions in the few-GeV region `http://conferences.fnal.gov/nuint07/`
[22] Aguilar-Arevalo A A *et al.* (MiniBooNE) 2007 (*Preprint* `arXiv:0706.0926[hep-ex]`)
[23] Espinal X and Sánchez F 2007 Measurement of the CCQE axial mass with the SciBar detector of K2K `https://indico.fnal.gov/materialDisplay.py?contribId=36&sessionId=9&materialId=slides&confId=804`
[24] Burkardt M 2003 *Int. J. Mod. Phys.* **A18** 173–208 (*Preprint* `hep-ph/0207047`)
[25] Ji X D 1997 *Phys. Rev. Lett.* **78** 610–613 (*Preprint* `hep-ph/9603249`)
[26] Airapetian A *et al.* (HERMES) 2007 *Phys. Rev.* **D75** 012007
[27] Ackerstaff K *et al.* (HERMES) 1999 *Phys. Lett.* **B464** 123–134 (*Preprint* `hep-ex/9906035`)